Electronic Supplementary Information (ESI) for

Highly Electron Deficient Tetrabenzoquinone Appended Ni(II) and Cu(II) Porphyrins: Spectral, Solvatochromism, Electrochemical Redox and Tuneable F^- and CN^- Sensing Properties

Pinki Rathi, Mandeep K. Chahal and Muniappan Sankar*

Department of Chemistry, Indian Institute of Technology Roorkee, Roorkee-247667, India

Table of contents

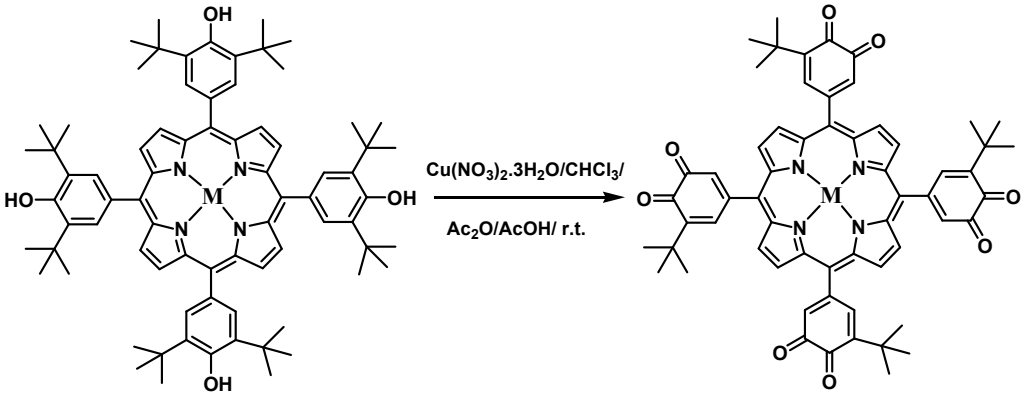

Scheme S1. Synthetic route for tetrabenzoquinone substituted Ni(II) and Cu(II)-porphyrins (**1** and **2**).

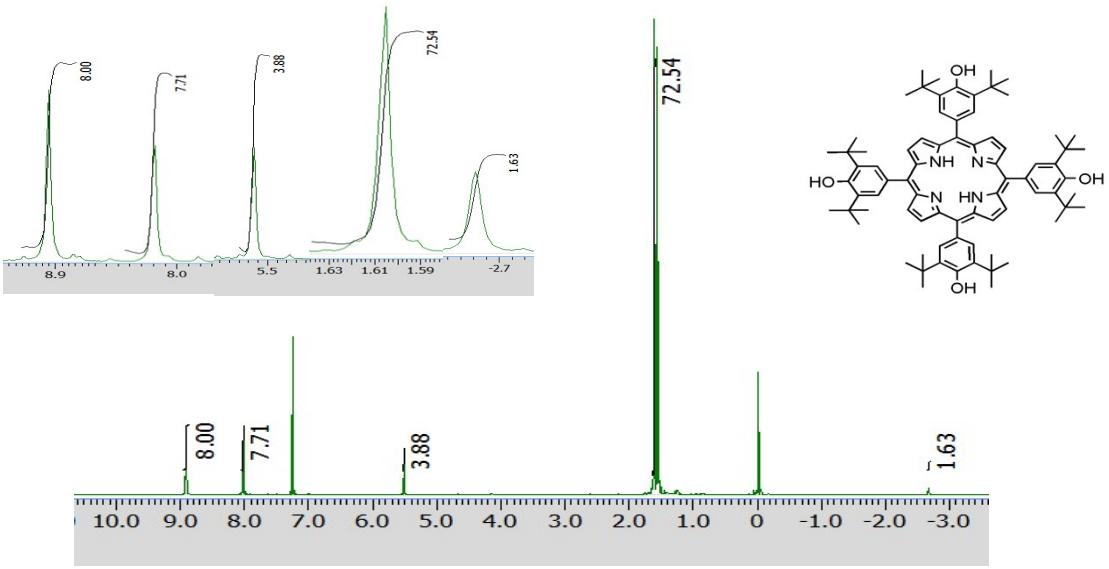

Figure S1. ^{1}H NMR spectrum of *meso*-tetrakis(3,5-di-*tert*-butyl-4-hydroxyphenyl)porphyrin in $CDCl_3$ at 298K.

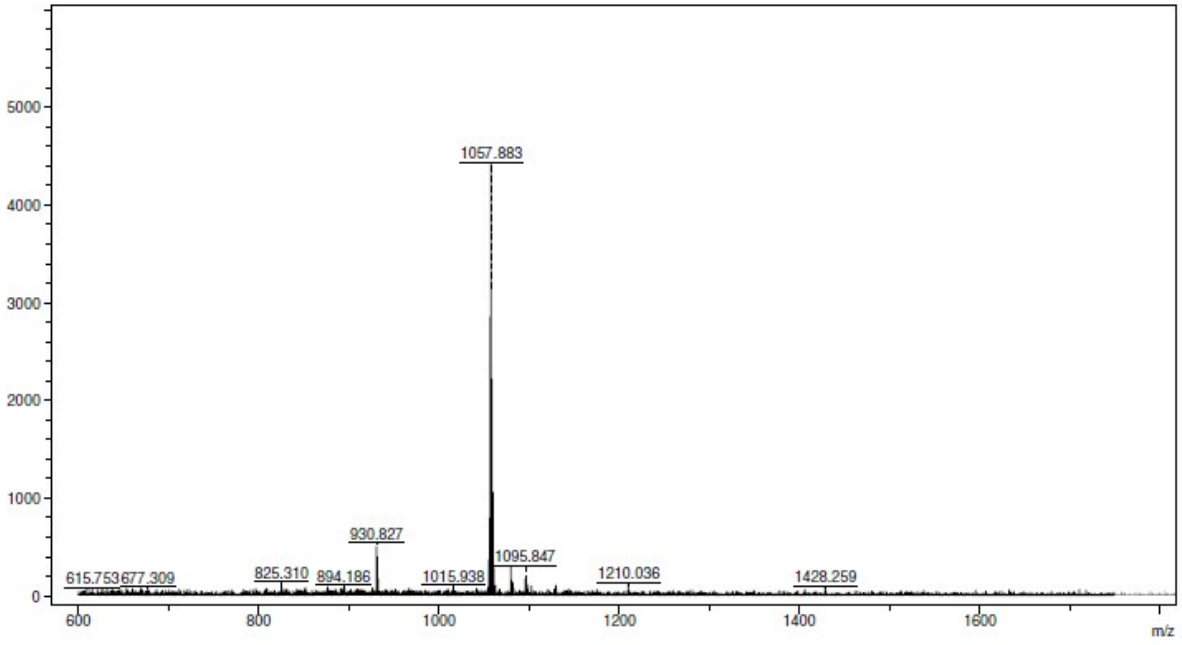

Figure S2. MALDI-TOF mass spectrum of *meso*-tetrakis(3,5-di-*tert*-butyl-4-hydroxyphenyl) porphyrin.

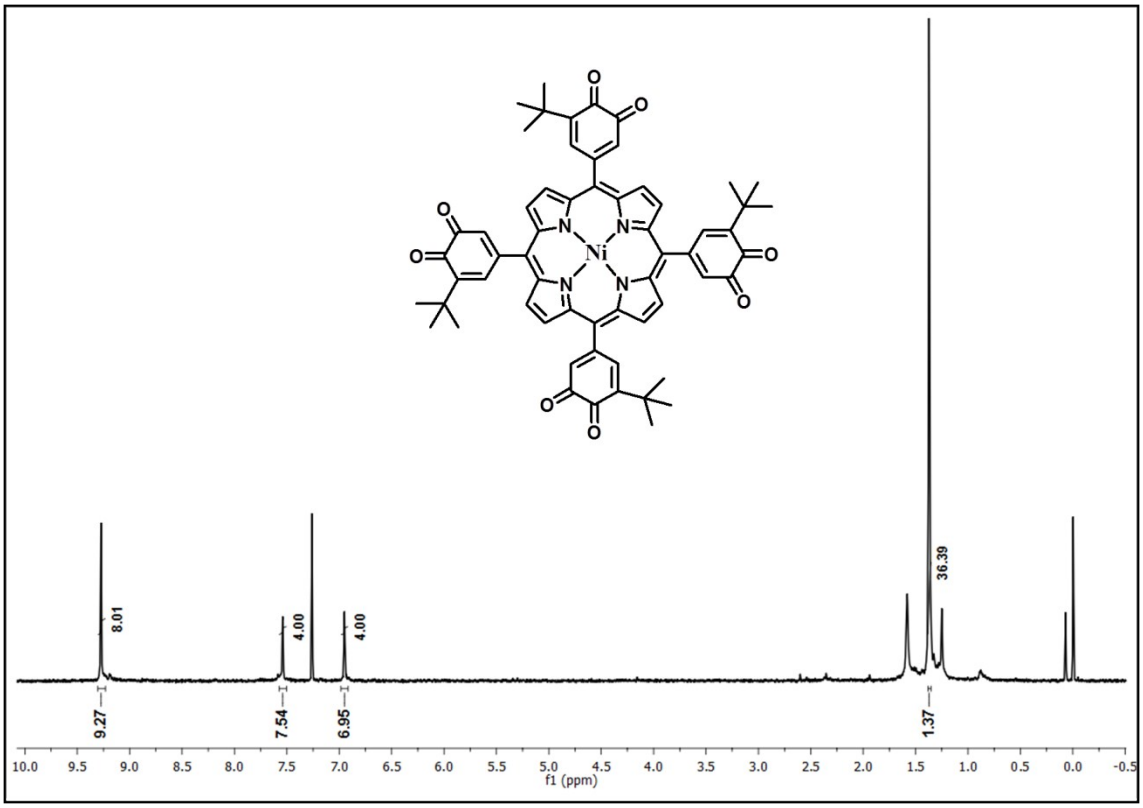

Figure S3. ^{1}H NMR spectrum of 5,10,15,20-tetrakis(3,4-dioxo-5-*t*-butylcyclohexa-1,5-dienyl)-porphyrinatonickel(II), Ni-diOxP (**1**) in $CDCl_3$ at 298K.

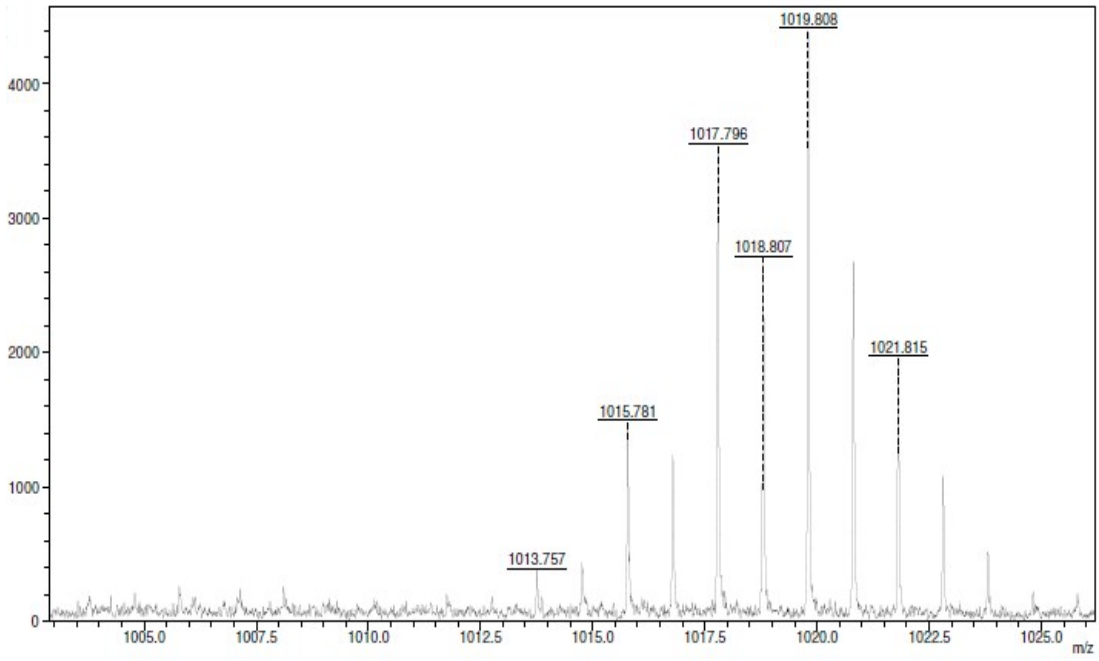

Figure S4. MALDI-TOF mass spectrum of Ni-diOxP (**1**).

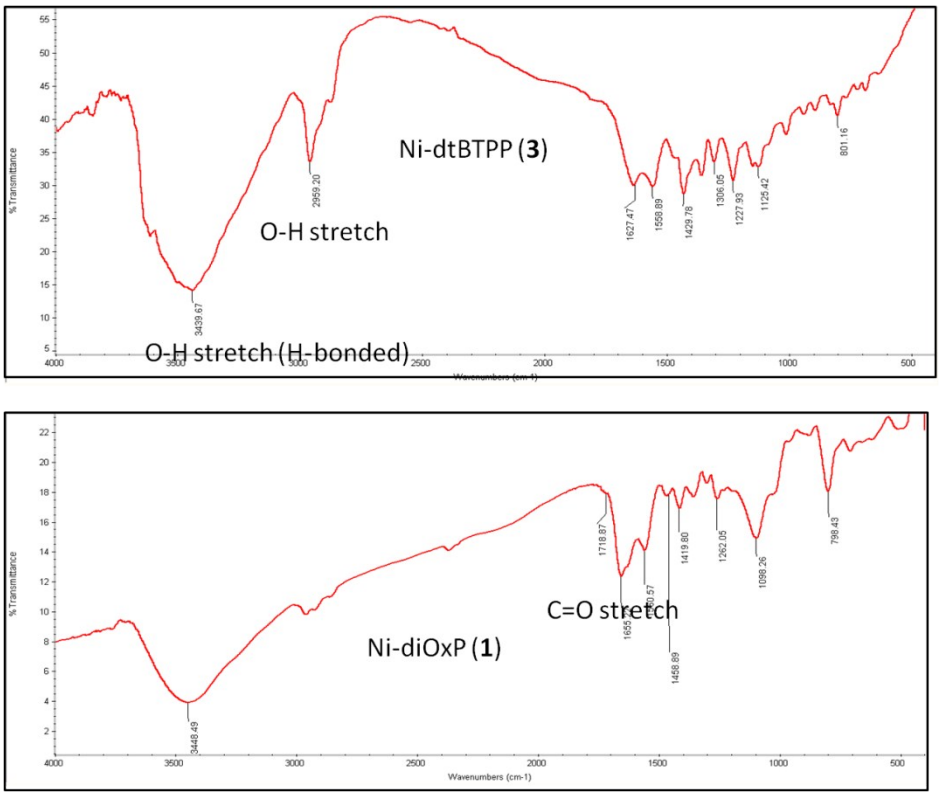

Figure S5. IR spectra of Ni-diOxP (**1**) and Ni-dtBTPP (**3**).

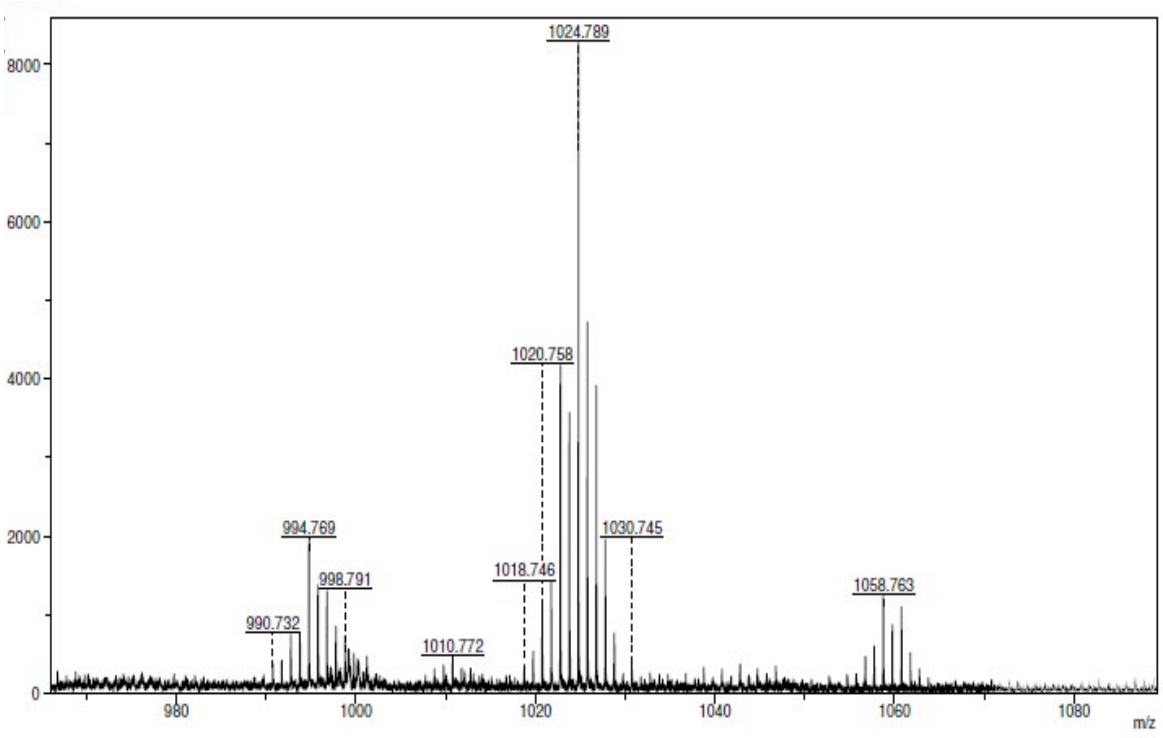

Figure S6. MALDI-TOF mass spectrum of Cu-diOxP (**2**).

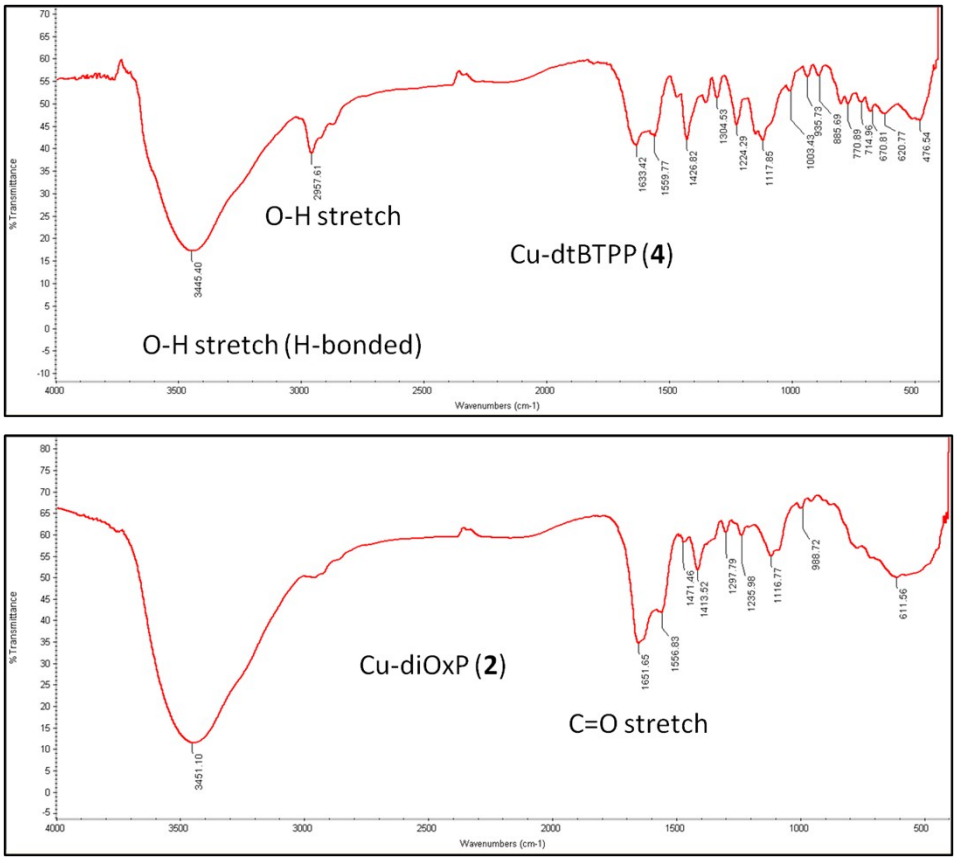

Figure S7. IR spectra of Cu-diOxP (**2**) and Cu-dtBTPP (**4**).

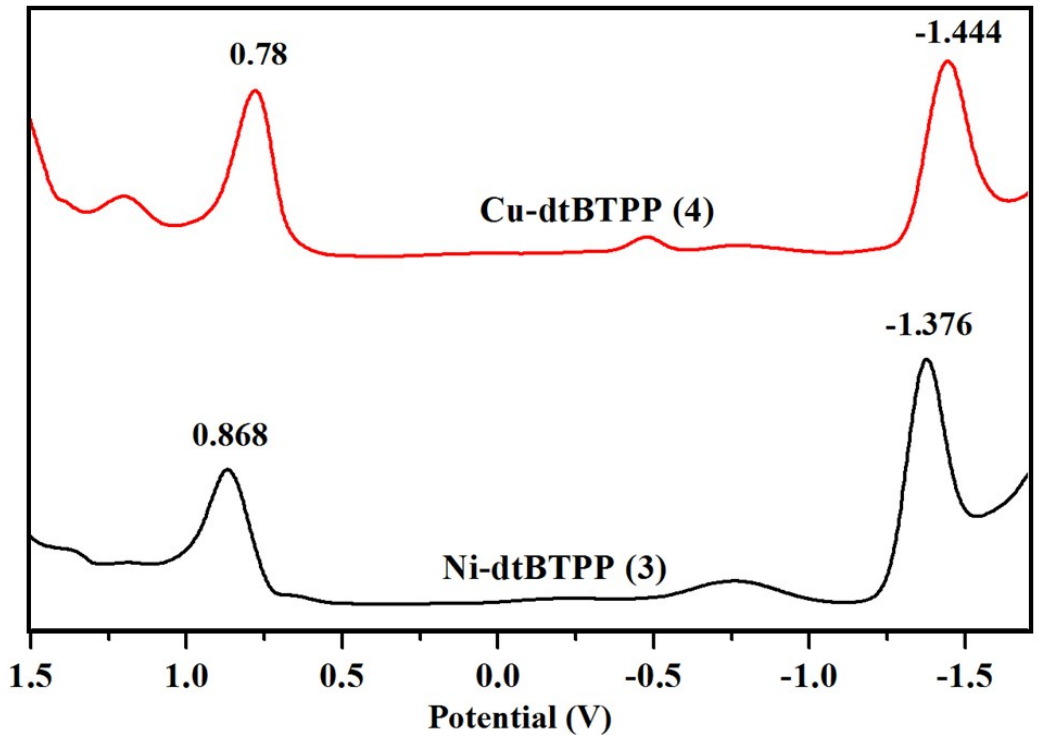

Figure S8. DPV traces of Ni-dtBTPP (**3**) and Cu-dtBTPP (**4**) in CH_2Cl_2 containing 0.1 M $TBAPF_6$ at 298 K.

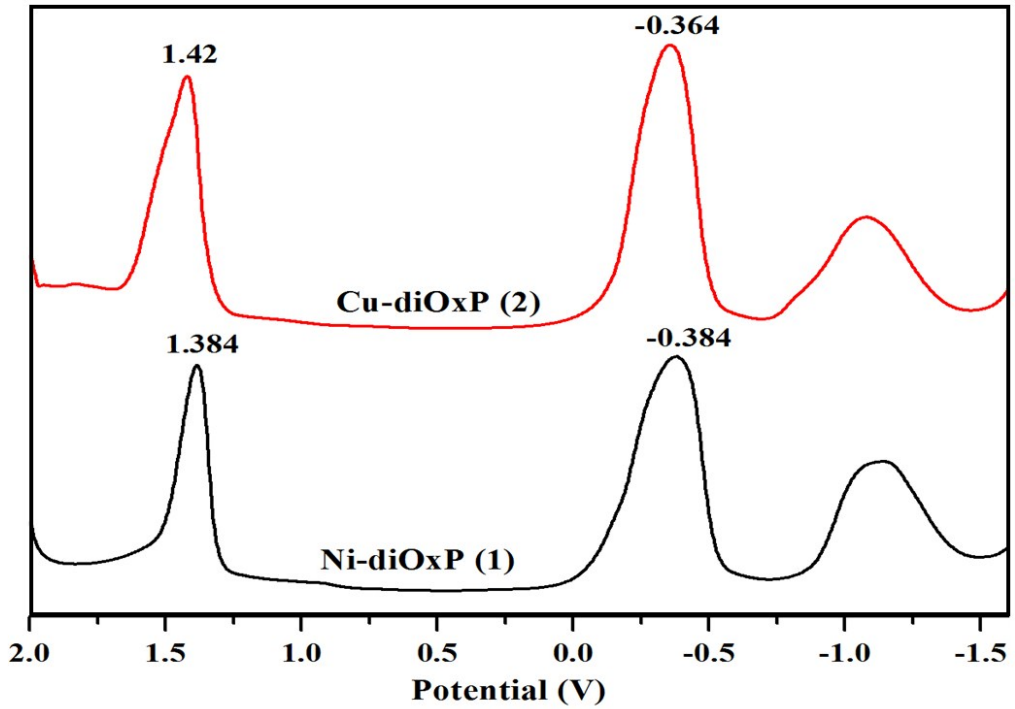

Figure S9. DPV traces of Ni-diOxP (**1**) and Cu-diOxP (**2**) in CH_2Cl_2 containing 0.1 M $TBAPF_6$ at 298 K.

Table S1. Electronic spectral data of Ni-diOxP (**1**) in different solvents at 298 K.

Solvent	B and Q bands, nm
CH_2Cl_2	397 (5.12), 501 (4.42), 611 (4.01)
Dimethyl Formamide	398 (5.04), 544 (4.16), 598 (3.97)
Acetone	394 (5.11), 543 (4.2), 600 (3.98)
DMSO	399 (5.07), 542 (4.22), 599 (4.00)
Toluene	402 (5.13), 506 (4.48), 609 (4.06)
Methanol	395 (5.1), 536 (4.23), 597 (4.03)
1,4-Dioxane	398 (4.97), 549 (4.12)
1,2-Dichlorobenzene (1,2-DCB)	400 (5.1), 504 (4.42), 620 (4.08)
Ethanol	398 (4.89), 500 (4.24), 610 (3.92)
Triehylamine	426 (5.14), 534 (4.14)
Piperdine	441 (5.13), 539 (4.03), 615 (3.83)
Chloroform	398 (5.1), 505 (4.42), 617 (4.04)
Pyridine	415 (5.05), 552 (4.21), 705 (3.88)
1,1,2,2-Tetrachloroethane (1,1,2,2-TCE)	400 (5.13), 513 (4.41), 628 (4.08)

Table S2. Electronic spectral data of Cu-diOxP (**2**) in different solvents at 298 K.

Solvent	**B and Q bands, nm**
Ethyl acetate	398 (4.85), 557 (3.88), 610 (3.62)
Dimethyl formamide (DMF)	405 (4.85), 553 (3.88), 620 (3.62)
Acetone	398 (4.83), 558 (3.82), 614 (3.6)
DMSO	406 (4.83), 560 (3.88), 631 (3.69)
THF	401 (4.86), 560 (3.88), 618 (3.68)
Toluene	403 (4.72), 568 (3.81), 618 (3.7)
Methanol	401 (4.83), 562 (3.84), 622 (3.67)
1,4-dioxane	401 (4.81), 560 (3.87), 612 (3.67)
1,2-dichlorobenzene (1,2-DCB)	404 (4.86), 519 (4.1), 642 (3.74)
Ethanol	402 (4.83), 555 (3.94), 626 (3.76)
Triehylamine	424 (4.96), 543 (3.87), 585 (3.28)
Piperdine	435 (4.9), 554 (3.88), 600 (3.49)
Chloroform	401 (4.94), 509 (4.15), 630(3.76)
Pyridine	410 (4.77), 568 (3.88), 642(3.67)
1,1,2,2-Tetrachloroethane (1,1,2,2-TCE)	402 (4.94), 518 (4.1), 638 (3.78)

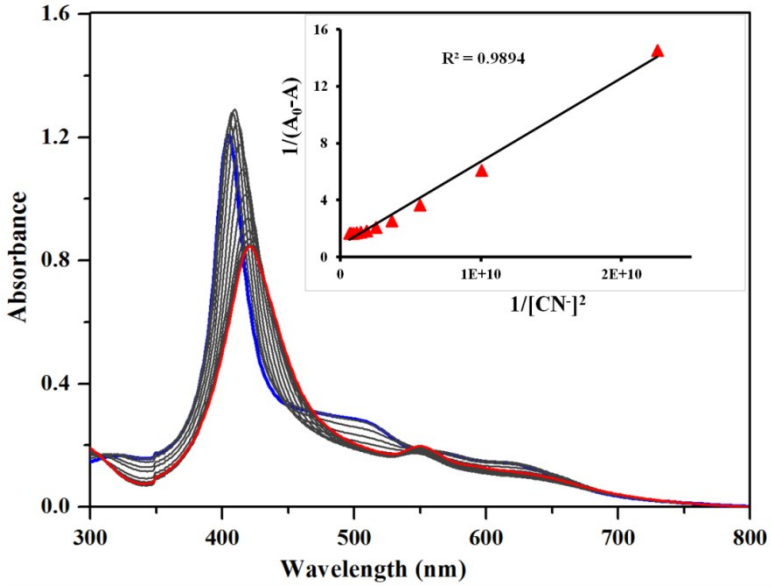

Figure S10. UV-Vis spectral response of **2** (3.15 X 10^{-5} M) upon incremental addition of CN^- (0- 4.78 × 10^{-5} M, 1.5 equiv.) in toluene. Inset shows BH-plot.

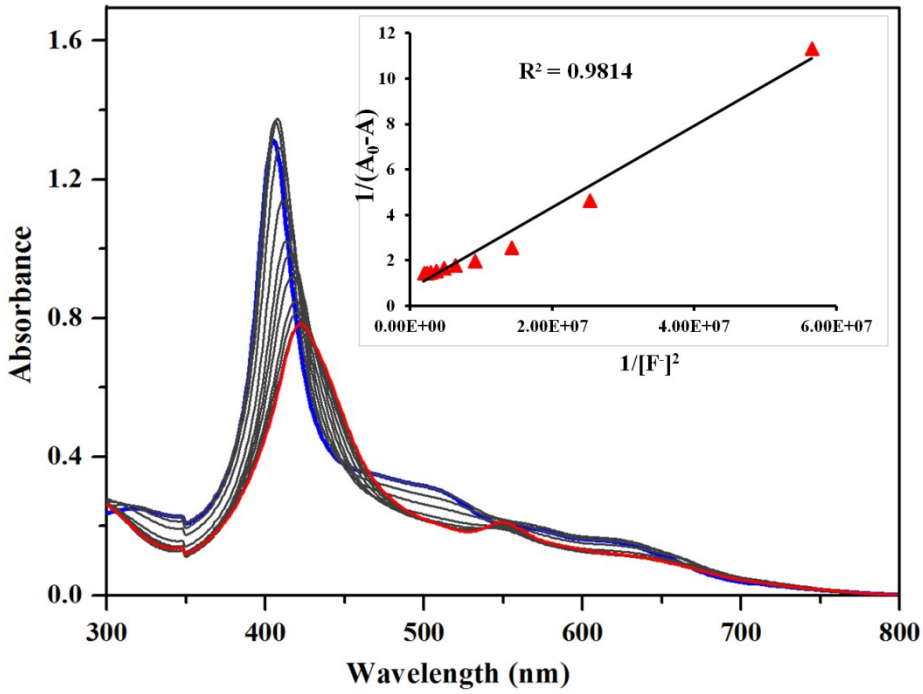

Figure S11. UV-Vis spectral response of **2** (3.15 X 10^{-5} M) upon incremental addition of F^- (0-7.29 × 10^{-4} M, 23 equiv.) in toluene. Inset shows BH-plot.

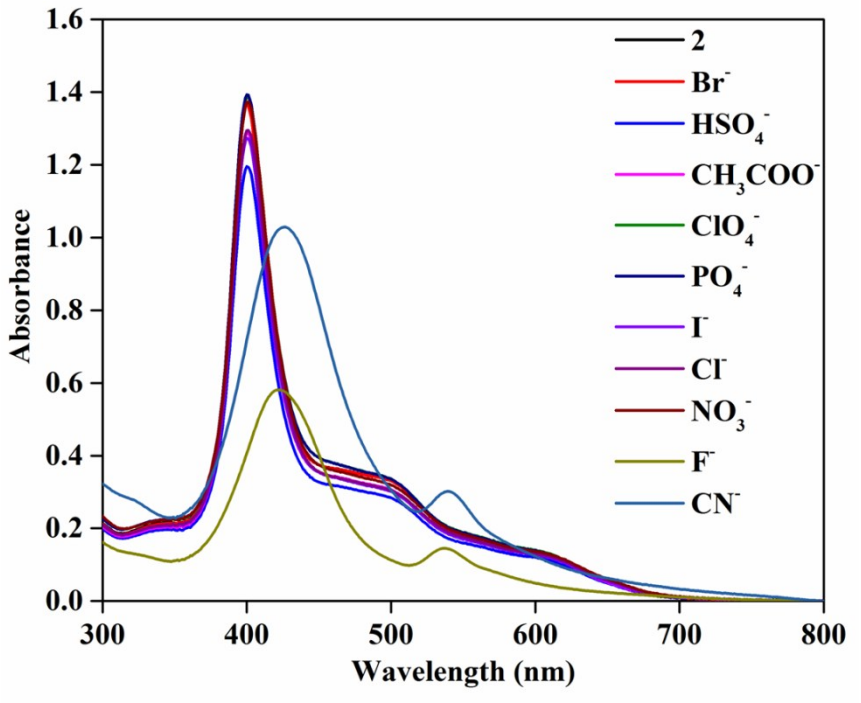

Figure S12. Absorption spectra of **2** (3.15×10^{-5} M) in the presence of different anions.

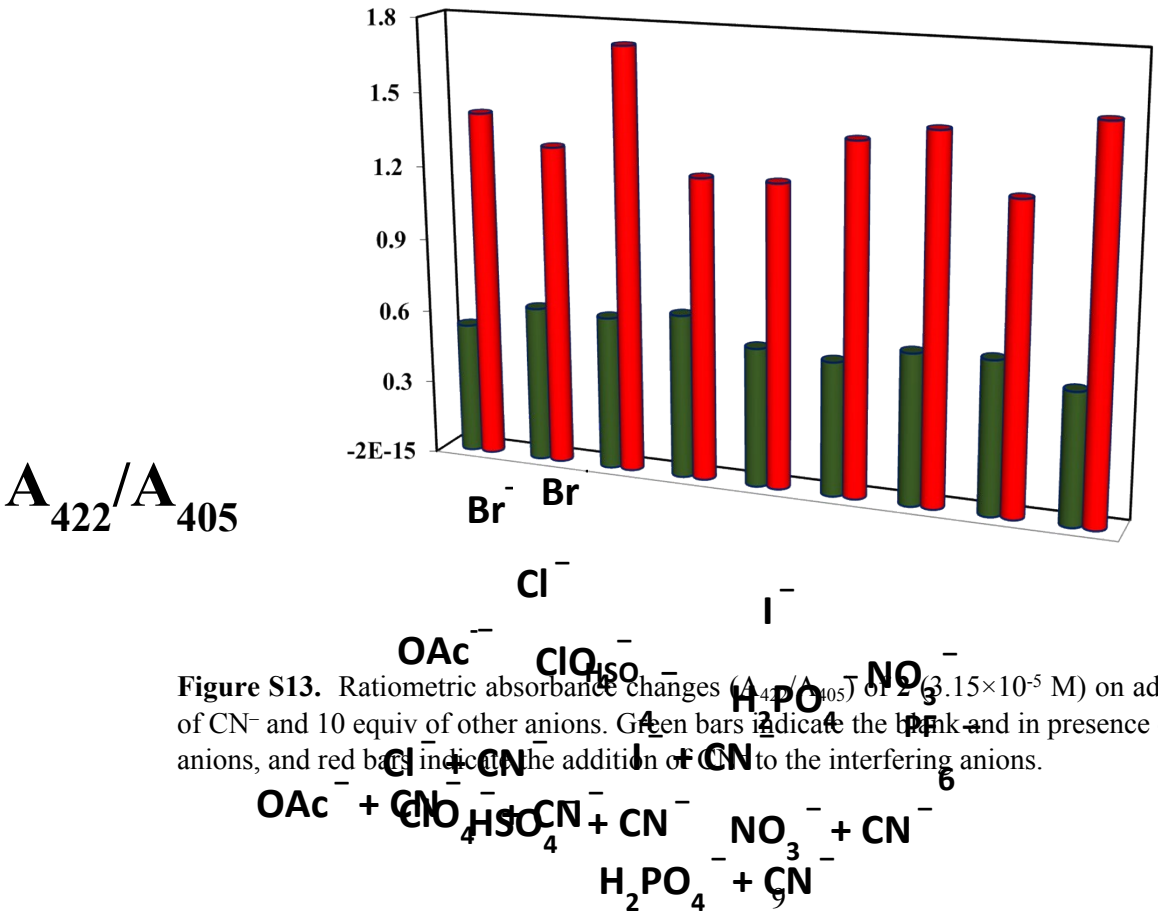

Figure S13. Ratiometric absorbance changes (A_{422}/A_{405}) of **2** (3.15×10^{-5} M) on addition of 1.5 equiv of CN^- and 10 equiv of other anions. Green bars indicate the blank and in presence of other interfering anions, and red bars indicate the addition of CN^- to the interfering anions.

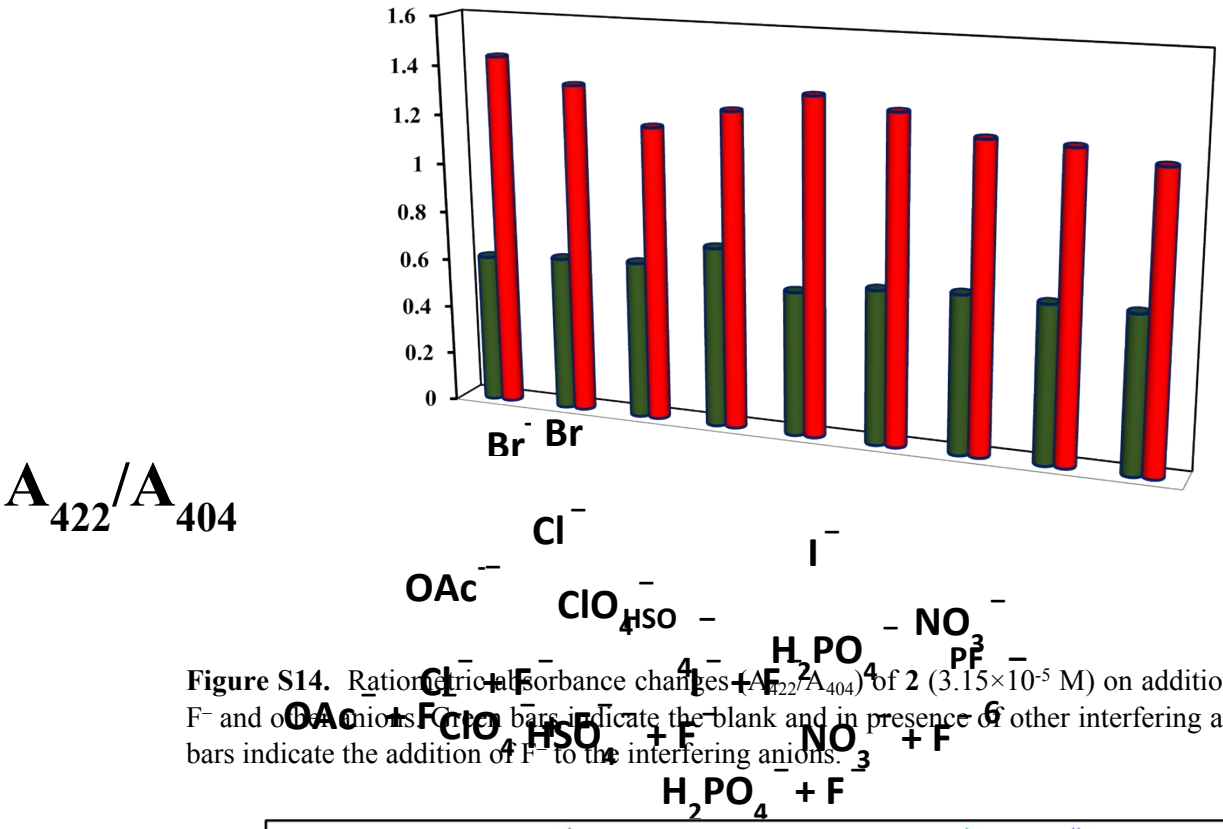

Figure S14. Ratiometric absorbance changes (A_{422}/A_{404}) of **2** (3.15×10^{-5} M) on addition of excees of F^- and other anions. Green bars indicate the blank and in presence of other interfering anions, and red bars indicate the addition of F^- to the interfering anions.

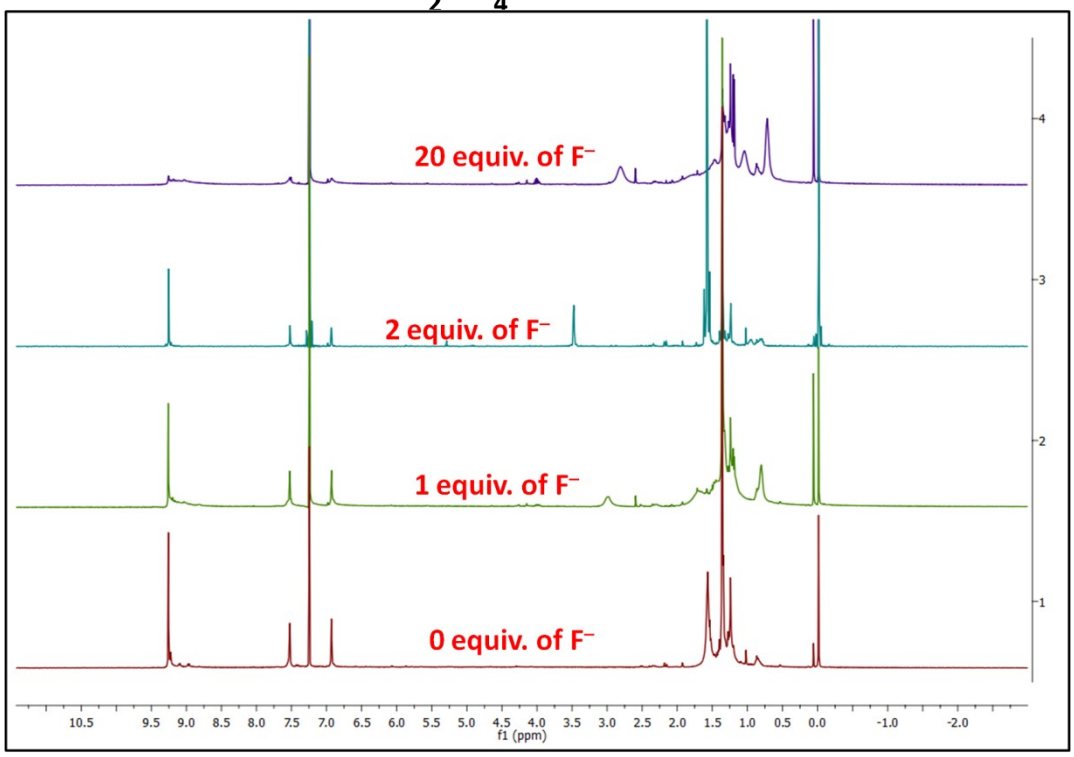

Figure S15. ^{1}H-NMR spectra of **1** in the absence and presence of F^- ions in $CDCl_3$.

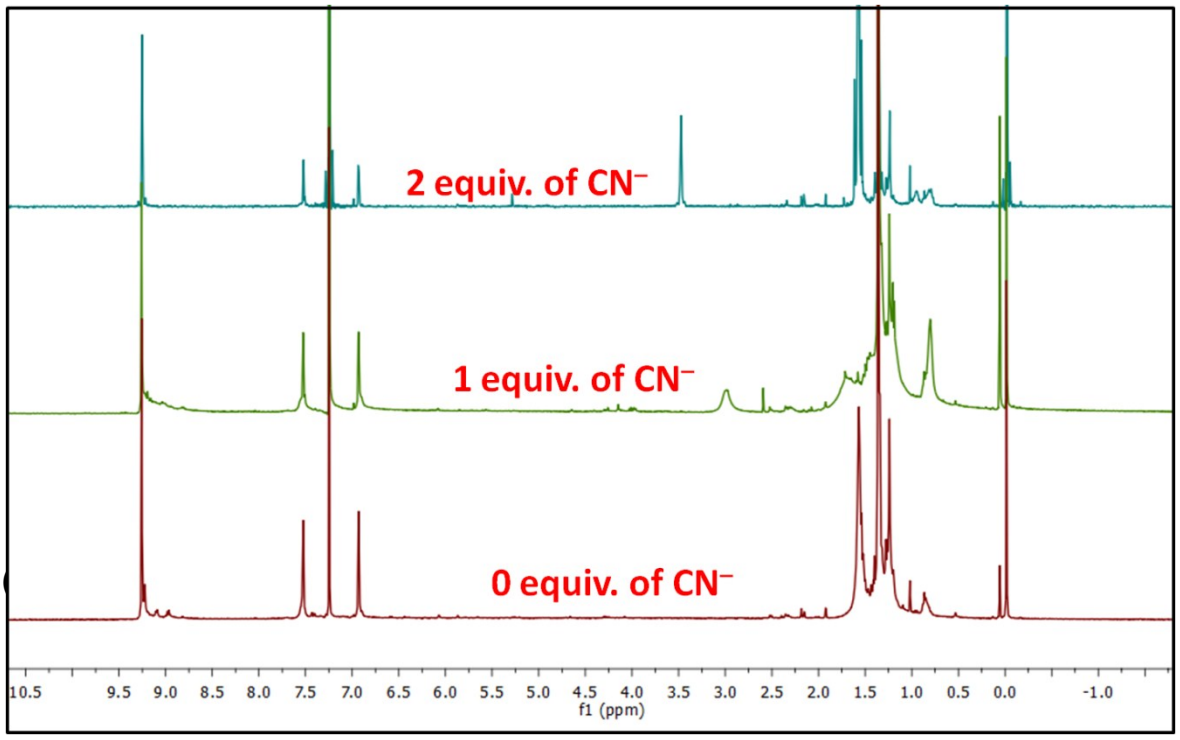

Figure S16. ^{1}H-NMR spectra of **1** in the absence and presence of CN^{-} ions in $CDCl_3$.

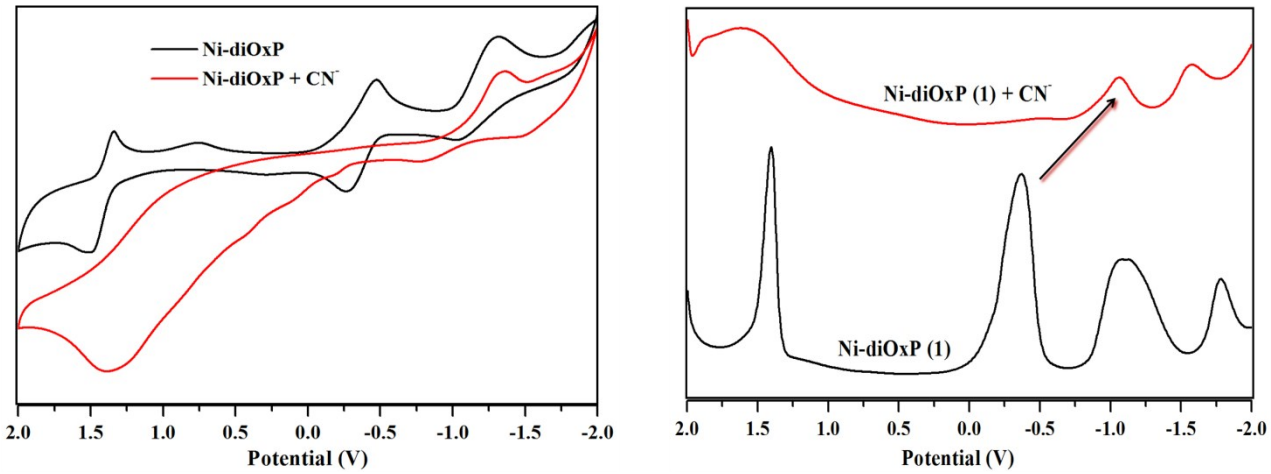

Figure S17. (a) Cyclic Voltametric (b) DPV (in V vs Ag/ AgCl) traces recorded for **1** (black) and **1**•2CN^{-} (red) in CH_2Cl_2 containing 0.1 M $TBAPF_6$ with a scan rate of 0.1 V/s at 298 K.

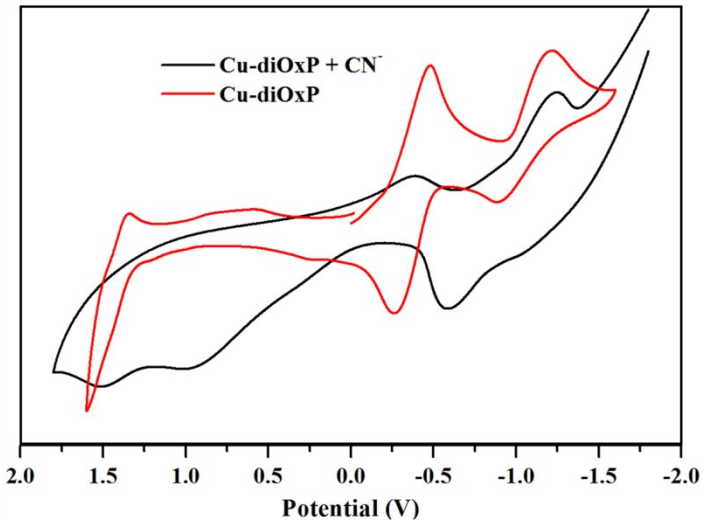

Figure S18. Cyclic Voltametric (in V vs Ag/ AgCl) traces recorded for **2** (black) and **2**•2CN^- (red) in CH_2Cl_2 containing 0.1 M $TBAPF_6$ with a scan rate of 0.1 V/s at 298 K.

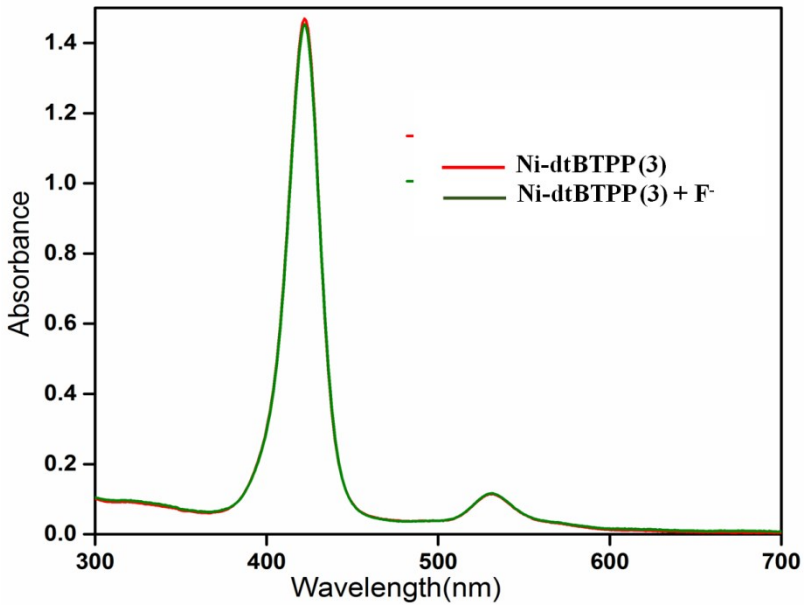

Figure S19. Absorption spectra of Ni-dtBTPP (**3**) in the absence and presence of 150 equiv. of fluoride ions.

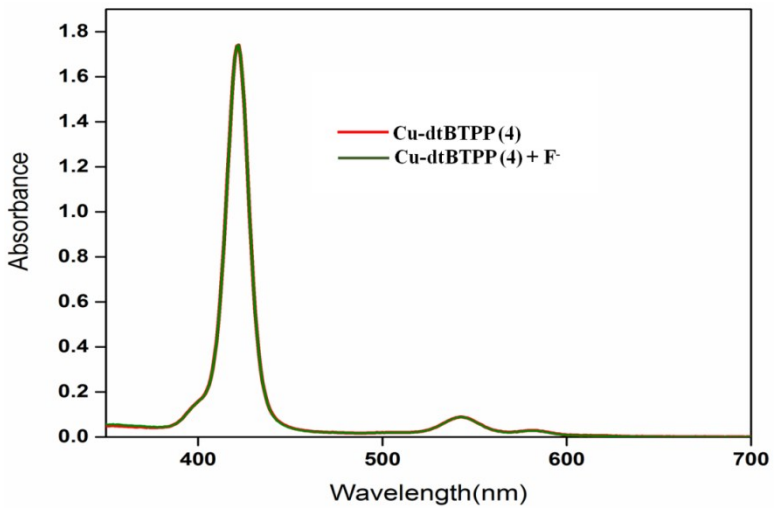

Figure S20. Absorption spectra of Cu-dtBTPP (**4**) in the absence and presence of 150 equiv. of fluoride ions.

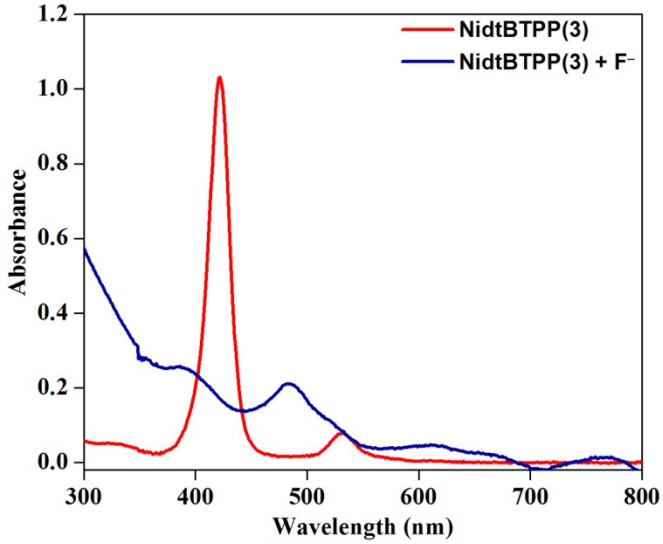

Figure S21. Absorption spectra of Ni-dtBTPP (**3**) in the absence and presence of >200 equiv. of fluoride ions.

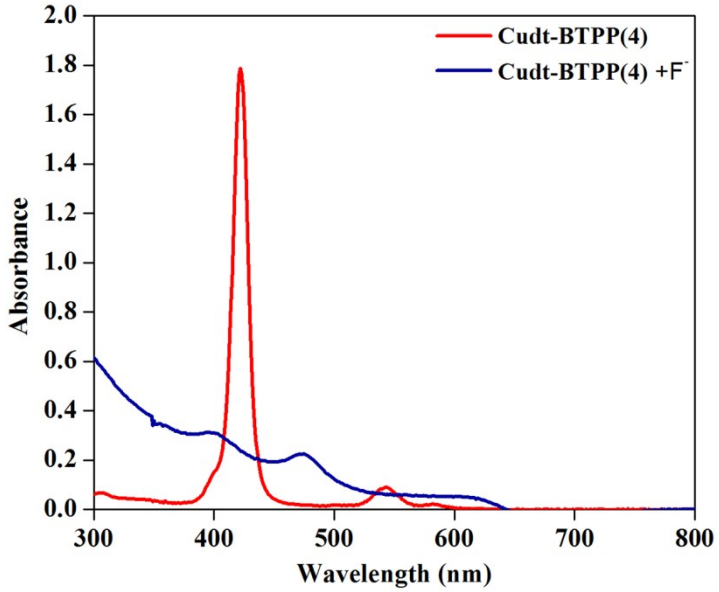

Figure S22. Absorption spectra of Cu-dtBTPP (**4**) in the absence and presence of >200 equiv. of fluoride ions.

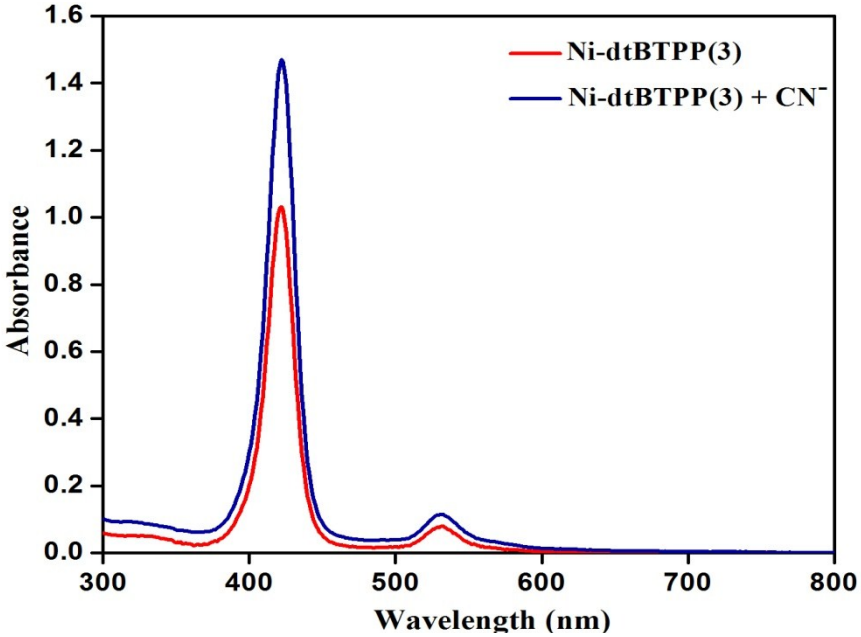

Figure S23. Absorption spectra of Ni-dtBTPP (**3**) in the absence and presence of >200 equiv. of cyanide ions.

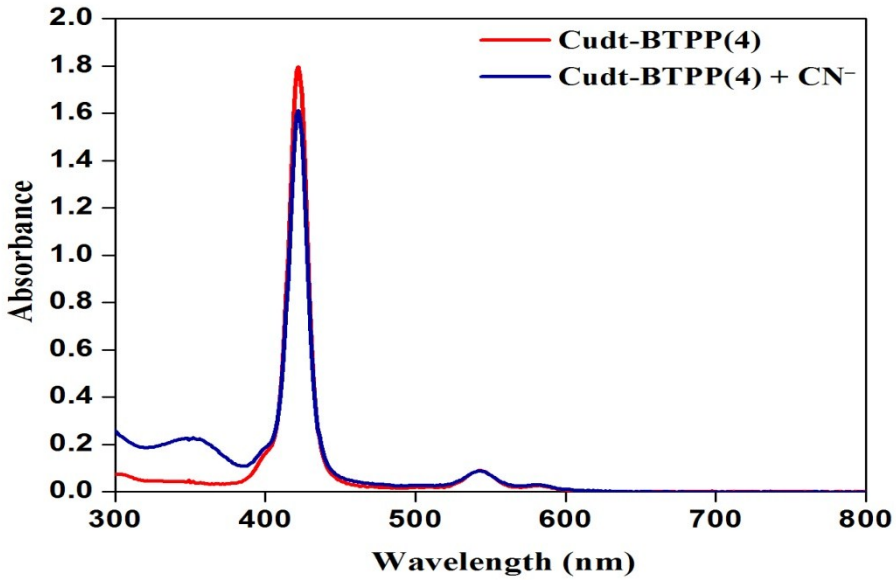

Figure S24. Absorption spectra of Cu-dtBTPP (**4**) in the absence and presence of >200 equiv. of cyanide ions.

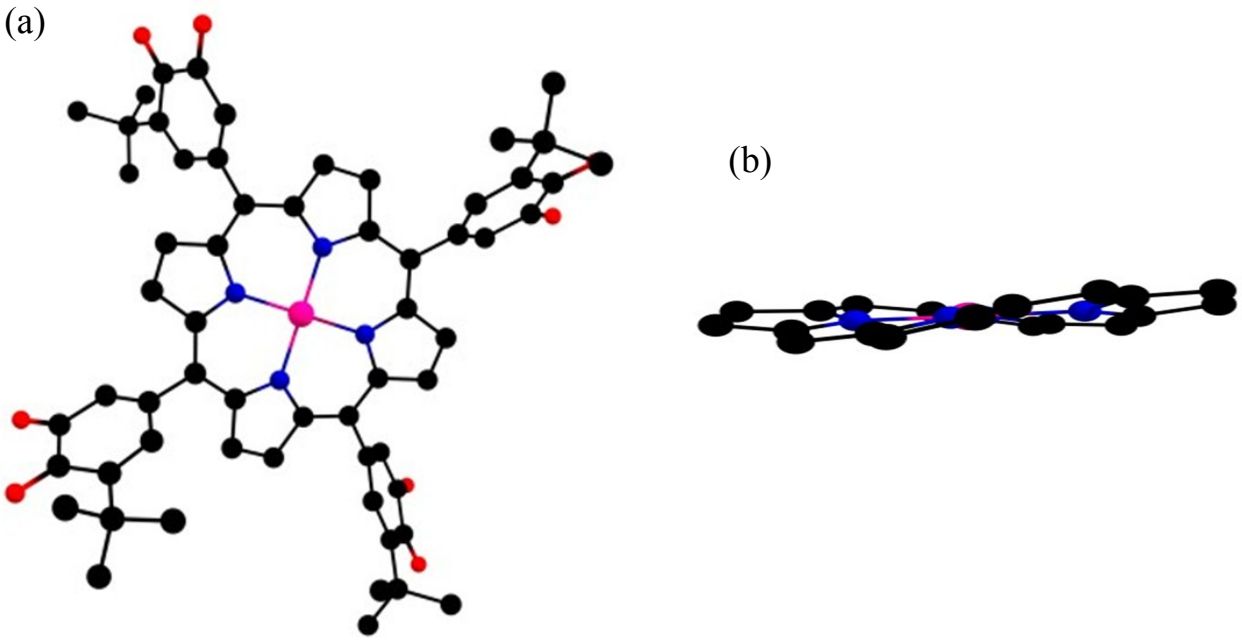

Figure S25. B3LYP/LANL2DZ-optimized geometry showing (a) top as well as (b) side views of Ni-diOxP (**1**); hydrogens are omitted for clarity. In the side view, the *meso*-phenyl substituents are not shown for clarity.

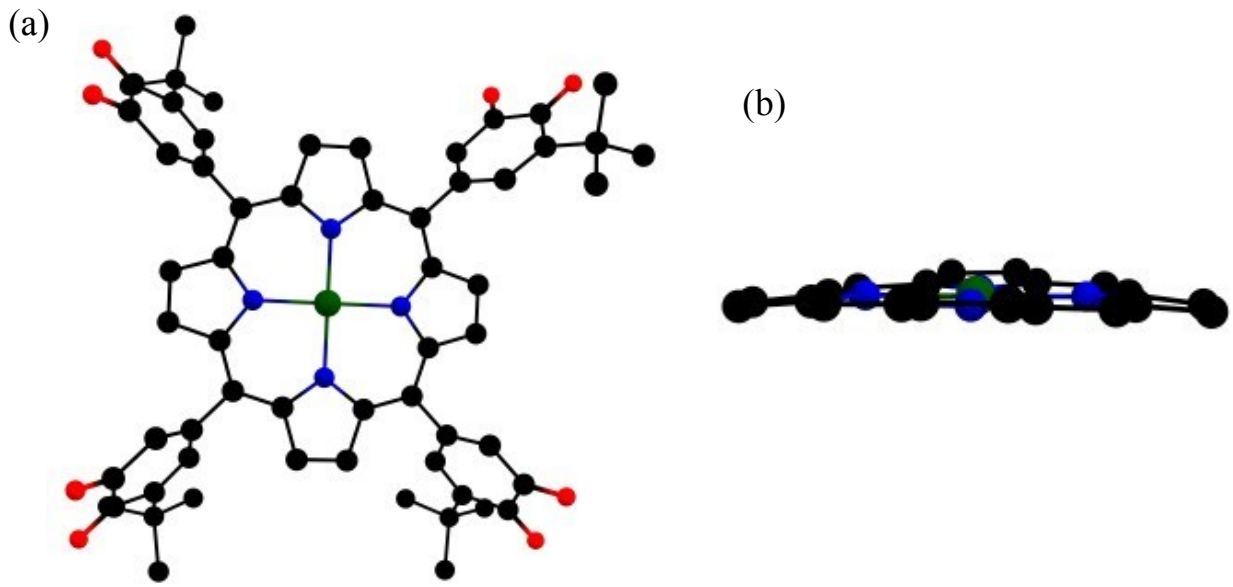

Figure S26. B3LYP/LANL2DZ-optimized geometry showing (a) top as well as (b) side views of Cu-diOxP (**2**); hydrogens are omitted for clarity. In the side view, the *meso*-phenyl substituents are not shown for clarity.

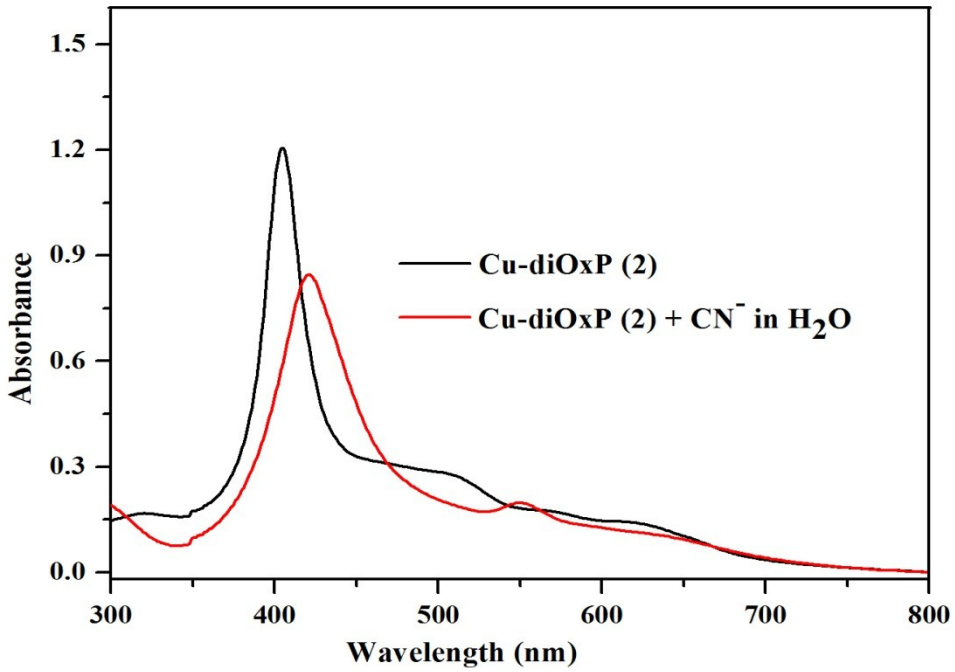

Figure S27. UV-vis spectra of Cu-diOxP (**2**) after addition of aqueous solution KCN and 18-crown-6.

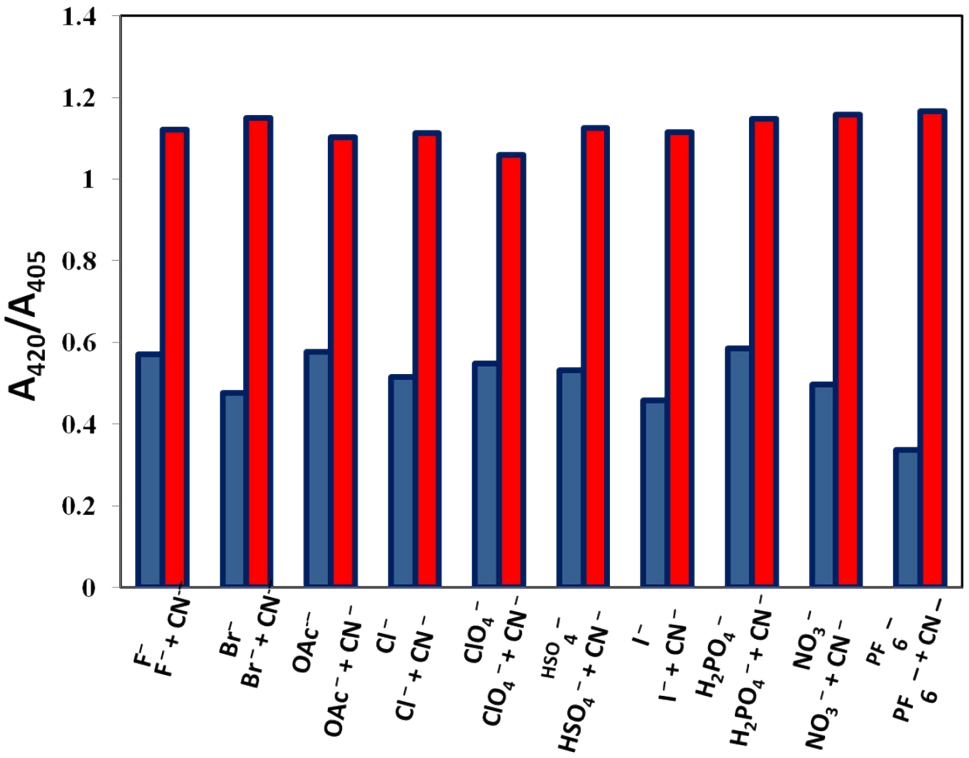

Figure S28. Ratiometric absorbance changes of **2** on addition of CN^- and 10 equiv excess of other anions in aqueous meium. Blue bars indicate the blank and in presence of other interfering anions, and red bars indicate the addition of CN^- to the interfering anions.

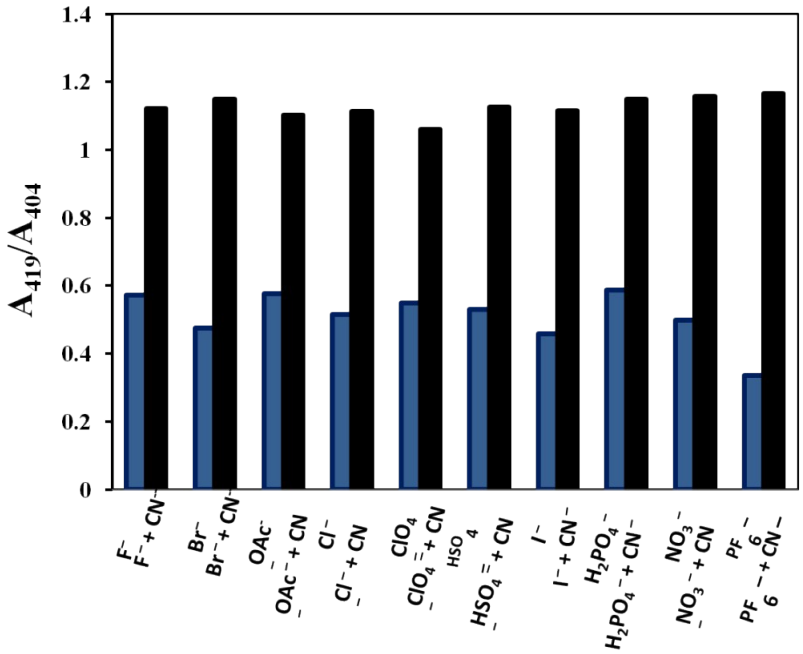

Figure S29. Ratiometric absorbance changes of **1** on addition of CN^- and 10 equiv excess of other anions in aqueous medium. Blue bars indicate the blank and in presence of other interfering anions, and black bars indicate the addition of CN^- to the interfering anions.